& DMPK 12(6) (2024) 925-942; doi: https://doi.org/10.5599/admet.2434

ADMET

Open Access : ISSN : 1848-7718

http://www.pub.iapchem.org/ojs/index.php/admet/index

Original scientific paper

Spray-dried cyclophosphamide-loaded polyhydroxyalkanoate microparticles: design and characterization

Sergei Lipaikin[1,*], Aleksei Dorokhin[1], Galina Ryltseva[1], Andrey Oberenko[1], Evgeniy Kiselev[1,2], Alexander Shabanov[3], Tatiana Volova[1,2] and Ekaterina Shishatskaya[1]

[1]*Siberian Federal University, 79 Svobodny pr., Krasnoyarsk 660041, Russia*
[2]*Institute of Biophysics SB RAS, Federal Research Center "Krasnoyarsk Science Center SB RAS", 50/50 Akademgorodok, Krasnoyarsk 660036, Russia*
[3]*L.V. Kirensky Institute of Physics, Siberian Branch of the Russian Academy of Sciences, 50/12 Akademgorodok, Krasnoyarsk 660036, Russia*

*Corresponding Author: E-mail: *lipaikinsj@gmail.com*; *Tel.: +7-913-182-4683*

Received: May 15, 2024; Revised: September 28, 2024; Published: October 9, 2024

Abstract

Background and purpose: Cyclophosphamide (CP) is a widely used antitumor and immunosuppressive drug, but it is highly cytotoxic and has carcinogenic and teratogenic potential. To reduce adverse effects of CP therapy and the frequency of its administration, the microencapsulation of CP into biodegradable polymeric matrices can be performed. However, according to the literature, only a few polymers were found suitable to encapsulate CP and achieve its' sustained release. **Experimental approach**: In this research, spray-dried cyclophosphamide-loaded poly(3-hydroxybutyrate-co-3-hydroxyvalerate) (PHBV) microparticles were prepared and characterized in terms of their average hydrodynamic diameter, polydispersity index, surface morphology, zeta potential, encapsulation efficiency, drug loading, thermal properties and cytotoxicity against 3T3 cells. **Key results**: The obtained CP-loaded microparticles had a regular spherical shape, uniform size distribution with an average diameter of 4.21±0.04 µm and zeta potential of -34.2±0.2 mV. The encapsulation of cyclophosphamide into the PHBV matrix led to a decrease in melting and degradation temperatures and an increase in diameter, glass transition and cold crystallization temperatures compared to blank microparticles. Moreover, microencapsulation of cyclophosphamide lowered its cytotoxicity compared to the pure drug: the number of dead cells in the culture decreased by 28 %, while their metabolic activity increased by 20 %. The cumulative *in vitro* drug release studies showed a gradual release of CP up to 18 days, so the obtained microparticle formulation can be used as a sustained-release cyclophosphamide delivery system. **Conclusion**: In this research, a novel cyclophosphamide-loaded platform based on PHBV microparticles was established and characterized. Overall, this study offers promising prospects for cancer therapy in the future.

Keywords

Microencapsulation; drug loading; drug release

Introduction

Cyclophosphamide (CP) remains one of the most successful antineoplastic agents. Even today, since its synthesis in 1958 [1], cyclophosphamide is still widely used as a chemotherapeutic agent and as an immunosuppressive drug in blood and marrow transplantation. CP is used to treat various types of diseases like lymphoma, myeloma, sarcoma, breast cancer, ovarian cancer, leukaemia, *etc* [2-4]. The duration of

cyclophosphamide therapy depends on the type and severity of illness and can range from several days to several months [5,6] or even years [7,8].

Nevertheless, CP is highly cytotoxic and like other alkylating agents, it is toxic predominantly to rapidly proliferating cells and tissues such as the haematopoietic system, hair follicles and so on. Well-known side toxic effects of conventional doses of cyclophosphamide are nausea, alopecia, infertility, pulmonary fibrosis, bladder injury, *etc* [9,10]. Furthermore, CP has carcinogenic and teratogenic potential [4,11].

To decrease the frequency of administration and the cytotoxic effects of cyclophosphamide and to achieve its controlled and sustained release, the microencapsulation of CP into the polymer matrices can be performed. There are known liposome-encapsulated [12], polylactic and poly-ε-caprolactone [13] microstructural carriers, poly(D,L-lactide-co-glycolide) [14,15] and chitosan [16] microspherical carriers of cyclophosphamide. Nevertheless, according to the literature, no studies have been conducted on the formation of polyhydroxyalkanoate microparticles containing cyclophosphamide.

Polyhydroxyalkanoates (PHAs) are a group of thermoplastic biopolymers of natural origin that are currently regarded as promising alternatives to synthetic, indestructible plastics [17,18]. PHAs are biocompatible, completely biodegradable and environmentally friendly materials: renewable sources (for example, waste fish oils [19], waste cooking oils [20], lignocellulose biomass waste [21], *etc*.) and greenhouse gases [22] are used as substrates for bacterial synthesis of PHAs [23]. The family of PHAs includes approximately 150 different types of monomers, which are synthesized by various microorganisms and differ significantly from each other in terms of their physico-chemical properties [21].

The aim of the research is to obtain and investigate the properties of poly(3-hydroxybutyrate-co-3-hydroxyvalerate) microparticles containing cyclophosphamide.

Experimental

Materials

Microbial poly(3-hydroxybutyrate-co-3-hydroxyvalerate) (M_w = 490.8 kDa, 10 mol.% of 3-hydroxyvalerate) was produced at the laboratory of Biotechnology of new biomaterials of Siberian Federal University, Russian Federation [24]. Cyclophosphamide monohydrate, dichloromethane (DCM), trichloromethane (TCM), dimethyl sulfoxide (DMSO), sulphamic acid and sodium nitrite were purchased from Merck (Germany).

Dulbecco's Modified Eagle Medium (DMEM), 3-(4,5-dimethylthiazol-2-yl)-2,5-diphenyltetrazolium bromide (MTT) and ReadyProbes™ Cell Viability Imaging Kit were obtained from Thermo Scientific (USA). Fetal Bovine Serum (FBS) and antibiotic-antimycotic solution were purchased from Sigma-Aldrich (USA).

All reagents and solvents were of analytical grade and used as received without further purification. The water used was purified by Arium® Pro Ultrapure water system (Sartorius AG, Germany).

Preparation of PHBV microparticles

PHBV microparticles (MPs) were prepared by spray drying of PHBV/DCM solution using Büchi Mini Spray Dryer B-290 (BUCHI Laboratory Equipment, Switzerland). The operating parameters were set as follows: argon gas flow rate 35 $m^3\ h^{-1}$, PHBV/DCM solution 0.1 % (w/v), inlet temperature 100 °C, PHBV solution feed rate 7.5 mL min^{-1}. The resulting MPs were collected, weighted and kept at -20 °C for further subsequent use in experiments.

Cyclophosphamide-loaded microparticles (CP-MPs) were obtained under similar conditions, except that the PHBV/DCM solution contained CP (CP to PHBV ratio 1:10).

Yield of microparticles, particle size, size distribution and zeta potential

The total yield (Y / %) of microparticles was determined according to Equation (1):

$$Y = \frac{M_o}{M_i} \quad (1)$$

where M_o is the mass of the obtained microparticles and M_i is the total mass of PHBV and CP used in the synthesis.

To determine the average hydrodynamic particle diameter, polydispersity index (PDI) and zeta potential of the obtained microparticles, Zetasizer Nano ZS (Malvern, UK) was used. 0.3 mg of each sample was suspended in 2 mL of deionized water and sonicated at 30 W for 1 min before the measurements.

Scanning electron microscopy

The morphology of the obtained microparticles was studied using Scanning Electron Microscope SU3500 (Hitachi, Japan). To obtain high-quality SEM images (by increasing conductivity and promoting heat dissipation from polymer matrix), microparticles were coated with 5 nm platinum layer using Leica EM ACE200 (Leica Microsystems, Germany).

Determination of CP encapsulation efficiency and drug loading

The encapsulation efficiency (EE) and drug loading (DL) of CP were determined by ultraviolet-visible spectroscopy using Genesys 10S UV-Vis (Thermo Scientific, USA) according to the procedure described in [25]. Briefly, 10 mg of CP-MPs were dissolved in 1 mL of TCM, added to the solution containing 1 mL of water, 1 mL of 5 % (w/v) HCl, 1 mL of 20 % (w/v) $NaNO_2$ and heated in a water bath at 60-65 °C for 20 min. The solution was cooled under tap water and mixed with 5 mL of 15 % sulphamic acid and 2 mL of 20 % (w/v) NaOH. The resultant solution was transferred into a volumetric flask and filled up to the mark with water. The absorbance was measured at 325.0 nm against the blank solution. The amount of CP in microparticles was determined using the calibration curve.

The encapsulation efficiency (EE, %) was calculated according to Equation (2):

$$EE = \frac{M_1}{M_2} 100 \quad (2)$$

where M_1 is the mass of CP in CP-MPs and M_2 is the initial mass of CP.

Drug loading was calculated by Equation (3):

$$EE = \frac{M_1}{M_o} 100 \quad (3)$$

Thermal properties

The glass transition temperature (T_g), cold crystallization point (T_{cc}), melting point (T_m), and thermal degradation temperature (T_{deg}) of the microparticles were determined by differential scanning calorimetry (DSC) and thermogravimetric analysis (TGA). DSC analysis was carried out using a DSC-1 differential scanning calorimeter (Mettler Toledo, Switzerland). 3 - 5 mg of each sample was placed in an aluminium crucible and heated up to 200 °C at a rate of 5 °C min^{-1}, held at 200 °C for 1 min, then cooled to -20 °C (5 °C min^{-1}) and held for 4 min. Each sample was further reheated to 200 °C at a rate of 5 °C min^{-1}. TGA was performed using TGA 1 (Mettler Toledo, Switzerland). The samples (3 to 5 mg) were placed in a ceramic crucible and heated from 50 to 600 °C at a rate of 10 °C min^{-1}. DSC and TGA analyses were performed under a nitrogen atmosphere. Thermograms were analysed using the “StarE” software.

FTIR spectroscopy

Fourier transform infrared spectroscopy (FTIR) analysis of the obtained microparticles was performed using a FT-801 FTIR spectrometer ("SIMEKS", Russia). The samples were dissolved in TCM and left to

evaporate the solvent to form a thin film. The FTIR spectra of the polymer films were recorded at 400 to 4000 cm^{-1} at room temperature.

To analyze the functional groups on the surface of the obtained microparticles ATR-FTIR spectroscopy technique was performed using ATR-accessory for FT-801 FTIR spectrometer (ZnSe crystal).

Data acquisition is performed at a resolution of 4 cm^{-1}, employing 64 scans per spectrum.

In vitro release

The investigation of the release of CP from CP-MPs was carried out *in vitro*. For this purpose, 2 mg of CP-MPs samples were suspended in 2 mL of phosphate-buffered saline (pH 7.4) in a 2.5 mL sterile centrifuge tubes. The tubes were thermostated at 37 °C. At predetermined time intervals, the solution was withdrawn from the tube, centrifuged at 11000 rpm for 5 min, and the supernatant was collected and successively treated with HCl, $NaNO_2$, sulphamic acid and NaOH as mentioned above. The amount of CP released was determined by the measurement of the absorbance of the solution at 325.0 nm (using a calibration curve). All measurements were performed in triplicate. The percentage of CP released at each time point was calculated by dividing the data obtained at each time by the total amount of CP inside the microparticles.

In vitro cell viability and cytotoxicity assays

In vitro cell viability of 3T3 fibroblast cells was estimated in the presence of CP, MPs and CP-MPs. The cells were cultivated in DMEM with the addition of FBS and antibiotic-antimycotic solution in CO_2 incubator (Sanyo, Japan). 3T3 cells were incubated for 24 h with the initial concentration of $2 \cdot 10^4$ cells cm^{-2}. After incubation, the medium was replaced by a fresh culture medium containing CP, MPs and CP-MPs (the concentration of cyclophosphamide in each well containing CP and CP-MPs was in accordance with the article [26], where the EC_{50} of CP against 3T3 cells was determined to be 10.8 mmol L^{-1}).

For the MTT assay, cell suspension was incubated with the studied samples for 72 hours. Then, the medium was removed, 200 µL of MTT solution in DMEM (0.25 mg mL^{-1}) was added to each well and the cells were incubated for 4 h at 37 °C in a CO_2 incubator. The resulting formazan was dissolved in DMSO, and the absorbance was determined at 550 nm (the reference wavelength was 650 nm) using iMark Microplate Reader (Bio-Rad Laboratories, USA). Metabolic activity (as an indicator of cell viability) was calculated relative to untreated cells according to Equation (2):

$$\text{Metabolic activity} = \frac{A_{\text{test}}}{A_{\text{control}}} 100 \quad (4)$$

where A_{test} is the absorbance of the test sample and A_{control} is the absorbance of the control sample.

Cytotoxicity was studied using the ReadyProbes™ Cell Viability Imaging Kit (Thermo Fisher, USA) to perform double staining: Hoechst 33342 (nuclei of live cells, blue) and SYTOX Green (nuclei of dead cells, green). Images were obtained using Leica DM6000 B TL (BF) +Fluo digital microscope (Leica Microsystems, Germany). The number and percentage of viable cells were analysed using the open-source software ImageJ [27], and cell viability was determined as a percentage of untreated cells.

Each measurement was carried out in triplicate.

Results and discussion

In the present research both blank and cyclophosphamide-loaded poly(3-hydroxybutyrate-co-3-hydroxyvalerate) microparticles were successfully prepared by spray drying method. The following characteristics of the obtained microparticles were determined: average hydrodynamic diameter, surface morphology, zeta potential, encapsulation efficiency, drug loading, thermal properties and cytotoxicity against 3T3 fibroblast cells.

Size and size distribution

The size and size distribution determine the scope of application of microparticles as delivery systems [28-30]. The dimensional characteristics (average hydrodynamic diameter, PDI) of the obtained microparticles were determined using the dynamic light scattering (DLS) method. The average hydrodynamic diameters of MPs and CP-MPs were 1.35±0.02 μm (PDI = 0.12±0.01) and 4.21±0.04 μm (PDI = 0.22±0.02), respectively. The DLS results are consistent with the results of scanning electron microscopy (Figure 1).

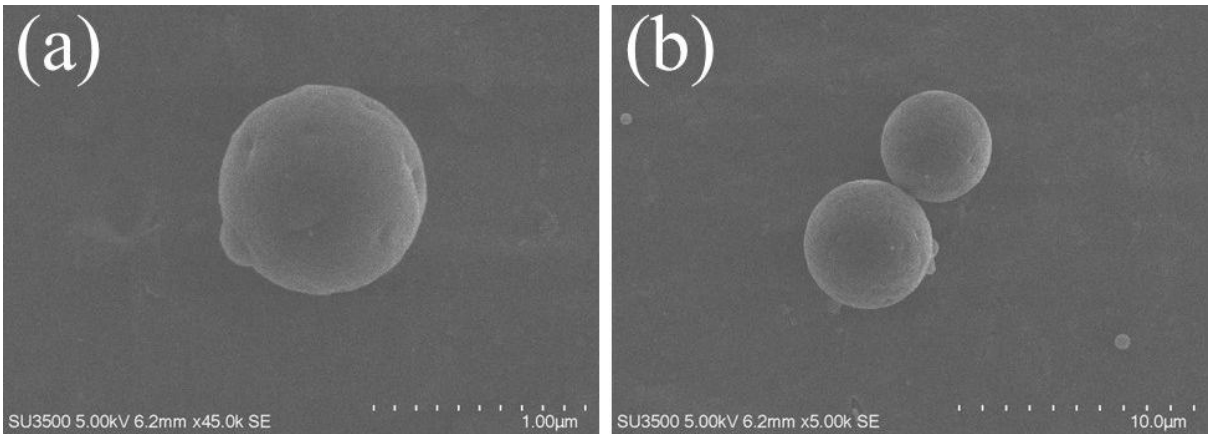

Figure 1. SEM images of the obtained microparticles: (a) MPs. (b) CP-MPs.

In general, an increase in the size of loaded PHBV-based microparticles compared to blank ones is a typical phenomenon, which is confirmed by the research of Dorokhin *et al.* (an increase in the average diameter of microparticles after encapsulation of rifampicin from 1.01 to 2.04 μm was noted) [31], Masood *et al.* (from 0.21 to 0.27 μm; ellipticine encapsulation) [32] and Vidal *et al.* (from 0.61 to 0.66 μm; quercetin encapsulation) [33]. An increase in the size of microparticles after encapsulation is also noted for microparticles based on PHA of other compositions [34-36].

The main routes of administration of CP are oral, intravenous and intramuscular [37]. It is known [38-41] that microparticles with a diameter of 5 to 8 μm are suitable for intramuscular administration (*e.g.* FDA-approved medication Lupron Depot® contains PLGA microparticles of approximately 8 μm in size [42]). Thereby, the obtained micronized form of cyclophosphamide can be suitable for this route of administration.

Zeta potential

The electrokinetic potential (zeta potential (ZP)) of a microparticle is the difference in the potential of the dispersion medium and the stationary layer of liquid surrounding the particle. The sign and value of the ZP allows to predict the applicability of microparticles in biological systems, as well as their tendency to aggregate. When microparticles are administered into the body, they are recognized as foreign material and are usually removed by the mononuclear phagocyte system [43]. The elimination of microparticles by the mononuclear phagocyte system tends to accelerate with the increase in surface charge [44].

It is considered that the zeta potential value exceeding 30 mV in absolute value is a marker of the aggregative stability of particles [45,46]. Moreover, the ZP of loaded microparticles may indicate the nature of encapsulation of the charged substance [47].

The zeta potentials of the obtained particles were determined to be -35.1±0.3 and -34.2±0.2 mV for MPs and CP-MPs, respectively, which indicates a good aggregative stability of the systems. Similar values of the zeta potentials are noted for various polymer carriers: Corrado *et al.* -35.1±0.3 mV (PHBHHx) [48], Murueva *et al.* -31.8±6.6 mV (P3HB) [49], Lipaikin *et al.* -39.6±0.4 mV (P3HB) [50], Xu *et al.* -31.0±1.4 mV (PLGA) [51], Ruan *et al.* -30.9±0.8 mV (PLA-PEG-PLA) [52].

It was noted that encapsulation of cyclophosphamide did not lead to any significant change in the zeta potential value, which may indicate the formation of microcapsules (the polymer matrix forms a membrane with a reservoir containing the encapsulated substance) or micromatrices (the encapsulated substance and polymer are evenly distributed throughout the volume of the microparticle). The interaction of the encapsulated drug with the surface of microparticles can affect ZP value.

Similar results were obtained by Shershneva *et al.* [53]: the encapsulation of tebuconazole of different concentrations into the P3HB matrix did not change the values of zeta potentials of microparticles. The values of ZPs were in the range from -32.6±0.9 to -35.7±2.0 mV.

Determination of CP encapsulation efficiency and drug loading

The encapsulation efficiency and the drug loading are the indicators of the success of the encapsulation process [54]. EE and DL values were determined spectrophotometrically.

The encapsulation efficiency and the cyclophosphamide loading into the PHBV-based matrix were 23.3±0.3 and 4.1±0.2 %, respectively. Similar values were noted in [55-57]. The relatively low EE and DL values may be caused by the fairly high crystallinity of PHBV (>60 %) [58,59].

The characteristics of the obtained microparticles are presented in Table 1.

Table 1. The characteristics of the obtained microparticles.

Sample	*Y* / %	Hydrodynamic diameter, μm	ZP, mV	EE, %	DL, %	PDI
MPs	31.4±0.4	1.35±0.02	-35.1±0.3	_	_	0.12±0.01
CP-MPs	35.1±0.3	4.21±0.04	-34.2±0.2	23.2±0.3	4.1±0.2	0.22±0.02

EE and DL values vary significantly depending on the carrier used. For instance, the encapsulation of *Artemisia turcomanica* extract into niosomal formulations resulted in an EE of 71.21 %, as reported by Keshtmand *et al.* [60]. Similar EE values (81.43 and 84.28 %) were achieved by Li *et al*. [61] when encapsulating temozolomide and tetra(4-carboxyphenyl)porphyrin in liposomes. Nonetheless, drug encapsulation efficiency in polymeric carriers is generally considerably lower (Salmasi *et al*. [62] encapsulated doxorubicin in PLGA nanoparticles and achieved an EE of 26.66 %).

Thermal properties

The glass transition temperature, cold crystallization point, melting point and enthalpies of fusion and cold crystallization were determined by differential scanning calorimetry (Table 2) [63,64].

Table 2. The results of DSC (second heating for MPs and CP-MPs) and TGA analyses.

Sample	T_g / °C	T_{m1} / °C	ΔH_1 / J g^{-1}	T_{m2} / °C	ΔH_2 / J g^{-1}	T_{cc} / °C	ΔH_{cc} / J g^{-1}	T_{deg} / °C
CP	_	49.9	102.6	_	_	_	_	132.1
MPs	-0.78	134.3	13.0	145.5	41.8	57.8	-40.7	276.2
CP-MPs	0.91	132.3	4.1	140.8	32.7	67.3	-37.1	267.7

T_g - midpoint temperature according to ASTM E1356 and ISO 11357; T_m and T_{cc} - peak temperatures according to ISO 11357, T_{deg} - extrapolated onset temperature according to ISO 11358.

The CP thermogram (Figure 2, curve A) shows a melting peak at 49.9 °C (which corresponds to the literature data [65,66]). Subsequent heating of cyclophosphamide probably leads to degradation or evaporation of CP, as evidenced by a wide peak in the temperature range from 120 to 200 °C.

DSC thermograms for both types of microparticles recorded during the first heating cycle (Figure 2, curves B and C) are similar in shape but differ in the position of the melting peaks. Since the first heating cycle characterizes the initial state of the polymer samples, it is fair to assume that the T_m shift is caused by the different packing of the polymer chains during the micronization process.

As mentioned above, the thermal behaviour of the studied samples is affected by the orientation of the polymers during the micronization process, so it is important to perform the second heating cycle to estimate T_g, T_{cc} and T_g. DSC thermograms for both types of microparticles (Figure 2, curves D and E) are similar in shape and have almost the same positions of the melting peaks: 134.3 °C (T_{m2} = 145.5 °C) and 132.3 °C (T_{m2} = 140.8 °C) for MPs and CP-MPs, respectively. However, a noticeable shift in the position of the cold crystallization peak (57.8 °C for MPs and 67.3 °C for CP-MPs) and an increase in the glass transition temperature from -0.78 °C to 0.91 °C were noted. The changes in T_{cc} and T_g are associated with the effect of CP thermal decomposition products on the thermal properties of the polymer: decomposition of CP (132.1 °C) occurs directly in the polymer melting zone (132.2 °C).

It was noted that there is no melting peak of CP at the CP-MPs thermograms (Figure 2, curves B and C), which may be caused by CP amorphization during its encapsulation into microparticles.

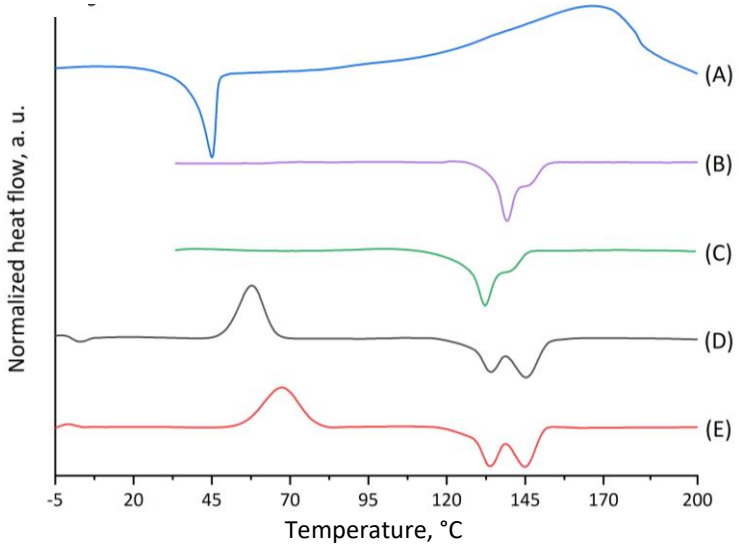

Figure 2. Normalized DSC thermograms of CP (A: 1st heating curve), MPs (B: 1st heating curve), CP-MPs (C: 1st heating curve), MPs (D: 2nd heating curve), CP-MPs (E: 2nd heating curve).

The thermal stability of CP, MPs, and CP-MPs was studied using thermogravimetric analysis. TGA curves and corresponding data for CP, MPs and CP-MPs are shown in Figure 3 and Table 2, respectively.

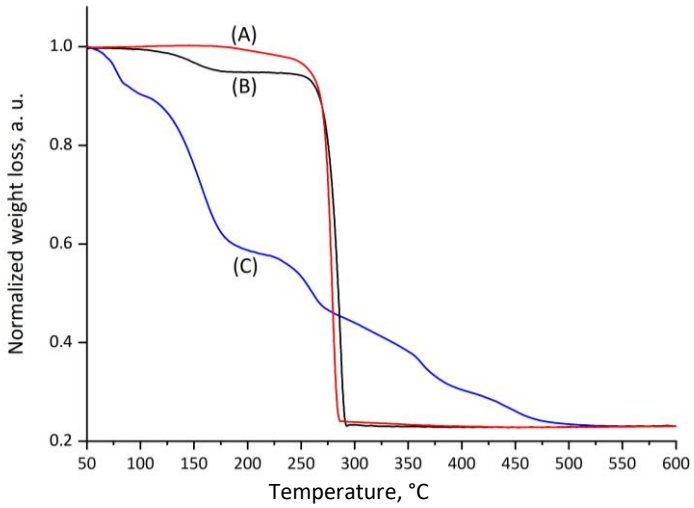

Figure 3. Normalized TGA thermograms of (A) CP-MPs, (B) MPs and (C) CP.

The TGA thermogram of CP shows several decomposition steps. At the first step (52.5 to 99.0 °C), a loss of 7.9 % of the sample mass (water loss) is noted. The next step (132.1 to 174.5 °C), where the degradation

rate reaches its maximum, is characterized by the loss of 25.8 % of mass, consistent with the DSC data. The total mass loss in the remaining areas is 20.7 %.

The thermal degradation of both types of microparticles showed two degradation steps. The first step is probably associated with the loss of residual DCM used in the preparation of microparticles.

The second step is typical for total PHA degradation [33,67]. The degradation temperature of CP-MPs is slightly lower than T_{deg} of unloaded microparticles (276.2 and 267.7 °C for MPs and CP-MPs, respectively). Such a decrease in T_{deg} of CP-MPs could potentially be caused by the influence of cyclophosphamide degradation products, which, at high temperatures, contribute to the accelerated degradation of the carrier. A decrease in T_{deg} of the polymer material was also noted in [68,69] after encapsulation of paclitaxel into the PLGA-PEG matrix and in [70] after encapsulation of metformin into PHBV-based microparticles.

FTIR spectroscopy

To confirm the fact of successful encapsulation of cyclophosphamide into the PHBV matrix, FTIR spectra of pure cyclophosphamide monohydrate and both types of microparticles (MPs, CP-MPs) were obtained (Figure 4). The absence of new absorption bands in the FTIR spectrum of CP-MPs compared to spectra of CP and MPs indicates no chemical interaction between cyclophosphamide and PHBV.

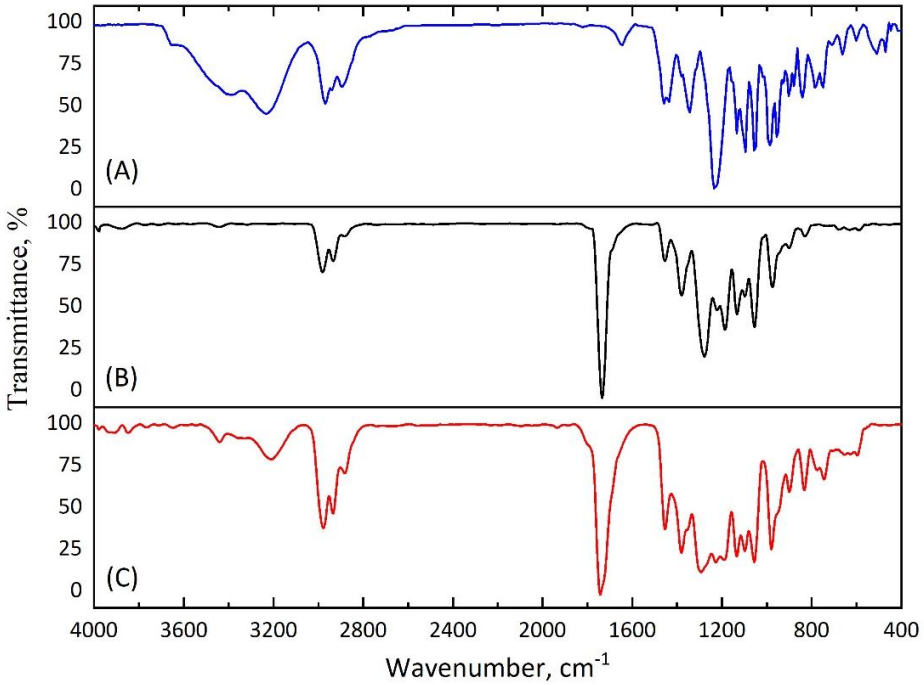

Figure 4. FTIR spectra of (A) CP, (B) MPs and (C) CP-MPs.

The success of encapsulation is evidenced by the appearance of the absorption bands in the FTIR spectrum of CP-MPs corresponding to the structural elements of cyclophosphamide: 3440 cm^{-1} (N-H), 1451 cm^{-1} (P-O-C), 1148 cm^{-1} (P=O), 873 cm^{-1} (CH_2-Cl) [71]. Due to the low intensity of the corresponding absorption bands, they can be seen in the spectrum obtained by subtracting the matrix spectrum (MPs) from the film spectrum (CP-MPs) (Figure 5).

As a result of encapsulation, cyclophosphamide can be localized both inside microparticles, forming micromatrices or microcapsules, and/or on their surface. The adsorption of CP on the surface of microparticles would probably cause a noticeable change in the zeta potential of CP-MPs, however, the zeta potentials of MPs (-31.4±0.4 mV) and CP-MPs (-35.4±0.3 mV) do not differ significantly.

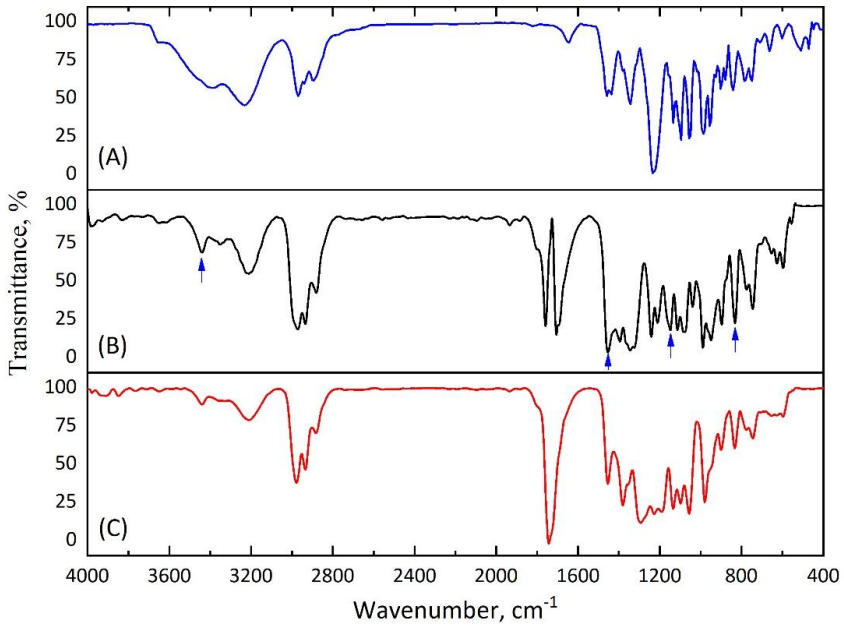

Figure 5. (A) FTIR spectrum of CP, (B) subtracted FTIR spectrum of MPs from CP-MPs and (C) FTIR spectrum of CP-MPs.

In order to confirm the absence of changes in the chemical structure of the MPs surface after CP encapsulation, the ATR-FTIR spectra of MPs and CP-MPs were obtained. As can be seen from Figure 6, there are no absorption bands of cyclophosphamide in the ATR-FTIR spectrum of CP-MPs and the positions of the absorption bands for both MPs and CP-MPs are completely identical. Thus, we suppose that CP is predominantly localized inside microparticles.

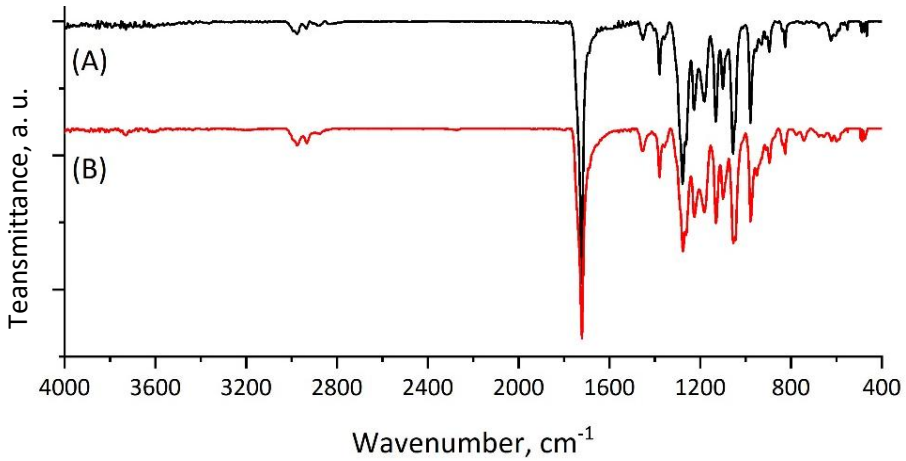

Figure 6. Normalized ATR-FTIR spectra of (A) MPs and (B) CP-MPs.

In vitro release

The release of CP from CP-MPs was investigated *in vitro* under physiological conditions (pH 7.4, 37 °C). *In vitro* drug release profile of cyclophosphamide from CP-MPs is presented in Figure 7.

Since PHA-based materials are hydrophobic and are not prone to hydrolytic degradation in the absence of enzymes or acids/bases [72], the dominant mechanism of the release of the encapsulated drug from PHA-MPs is diffusion [73]. The release of cyclophosphamide from CP-MPs has a two-stage pattern typical for systems based on polyhydroxyalkanoates [74,75]. At the initial stage of CP release, a slight burst effect caused by the desorption of cyclophosphamide from the surface of microparticles is observed. During the first 6 hours of exposure, about 12 % of the encapsulated substance is released. At the second stage, a slow release of the drug caused by the diffusion of CP to the surface of the MPs occurs. It was noted that the maximum

release of cyclophosphamide (62 %) was achieved in 432 hours (18 days), which correlates with literature data on the duration of cyclophosphamide therapy.

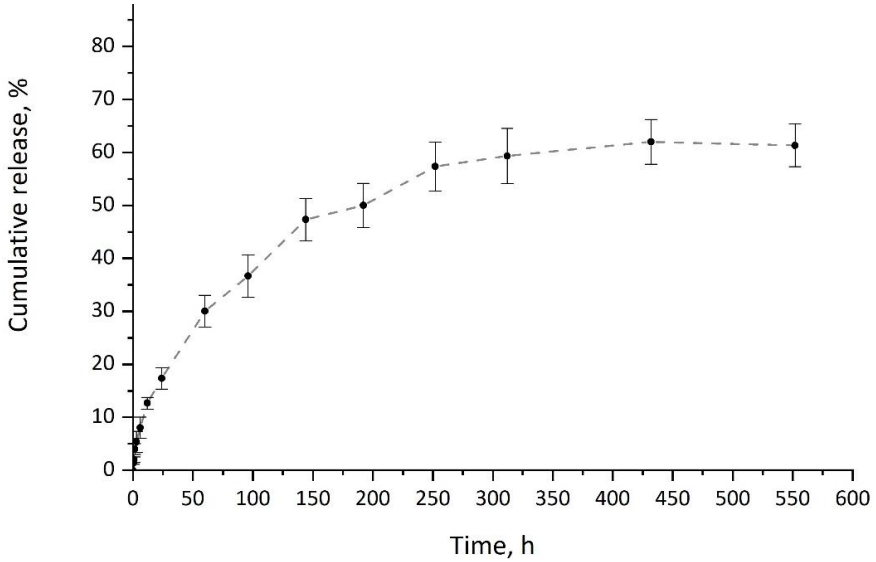

Figure 7. Release profile (kinetic curve) of CP-MPs.

Mathematical models such as zero-order, first-order, Higuchi and Hixson-Crowell were fitted to the *in vitro* release profile [76]. To determine the optimal model, the model with the highest coefficient of determination (R^2) was selected (Table 3) [77]. Based on this criterion, the Higuchi model was found to be best suited for the release kinetics of cyclophosphamide from CP-MPs (R^2 = 0.96), indicating that the release of CP from microparticles is controlled by Fickian diffusion [78].

Table 3. R^2 values of various drug release kinetic models.

Kinetic model	Zero-order	First-order	Higuchi	Hixson-Crowell
R^2	0.79	0.85	0.96	0.83

In vitro cell viability and cytotoxicity assays

The toxic effect of the micronized form of CP in comparison with unloaded microparticles and pure CP was estimated against fibroblast cell line 3T3.

According to the results of the MTT assay (Figure 8), the cultivation of fibroblasts with CP and CP-MPs resulted in a decrease in the number of viable cells.

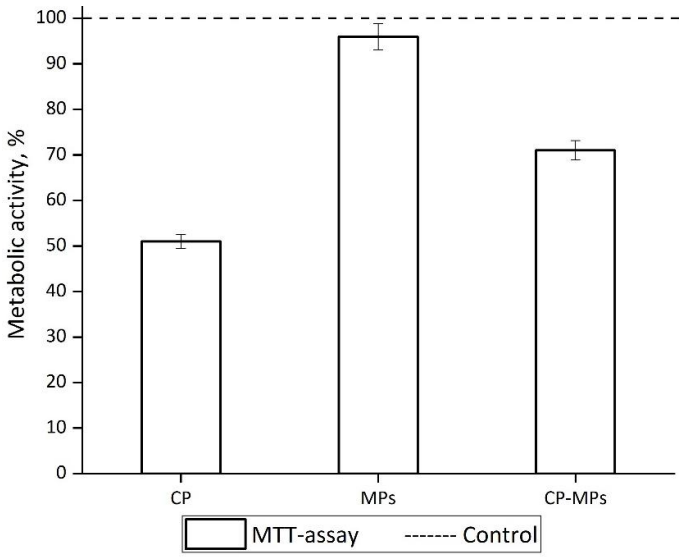

Figure 8. Metabolic activity of 3T3 cells in the presence of CP, MPs and CP-MPs.

The reduced toxic effect of CP-MPs may be associated with sustained release of the CP from the microparticles (according to the kinetic study, approximately 33 % of encapsulated cyclophosphamide is released over 3 days). The reduced cytotoxicity of microencapsulated forms of drugs is also noted in [79] in the case of encapsulating rifampicin into the PHBV matrix (V79 cells) and 5-fluorouracil into the PLGA matrix (MCF7 cells) [80]. The cultivation of cells with blank microparticles does not lead to a decrease in the metabolic activity of 3T3 in comparison with the untreated control culture.

Figure 9 shows the adhered fibroblasts after staining with Hoechst 33342 and SYTOX Green. Almost none of the dead fibroblasts (green in colour) could be identified during the cultivation with MPs. It means that MPs did not affect the viability of adherent cells compared to untreated control culture. In the case of cultivation 3T3 with CP and CP-MPs, 52 and 24 % of dead cells were found, respectively.

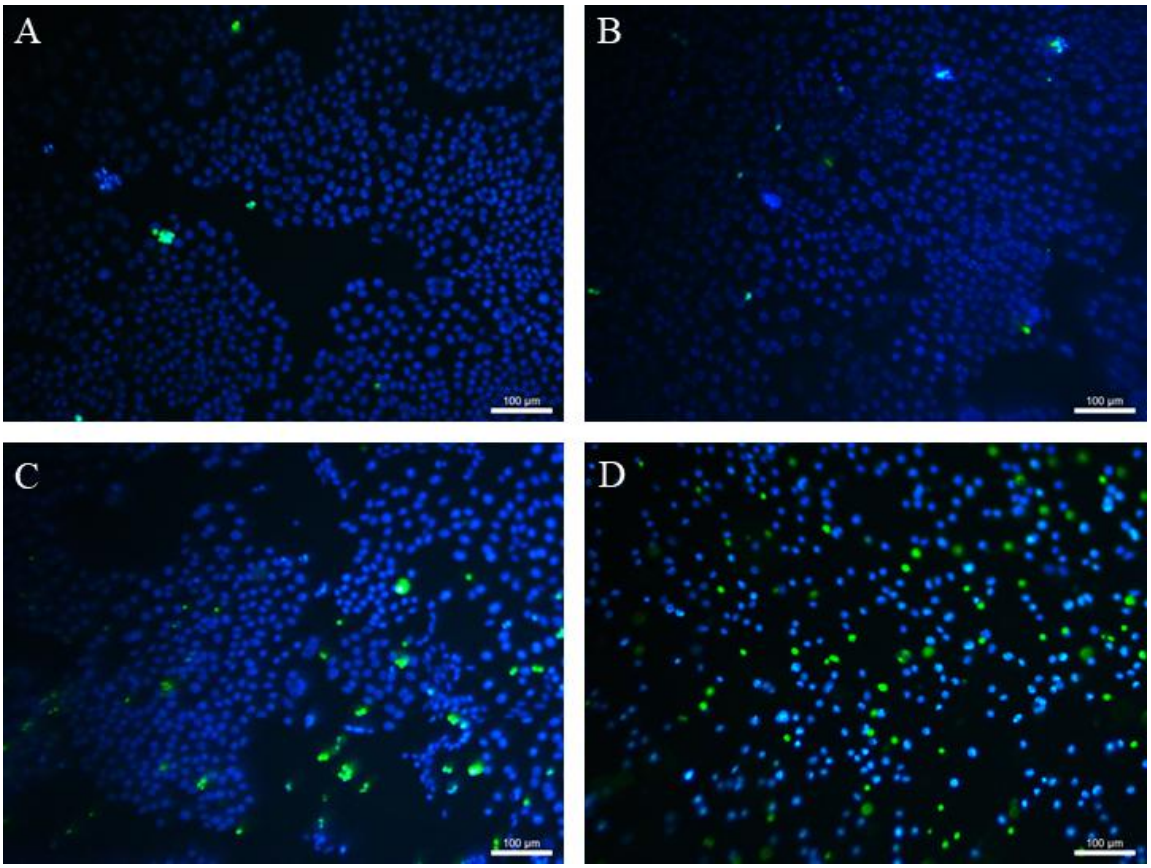

Figure 9. *In vitro* LIVE/DEAD assay: (A) control, (B) MPs. (C) CP-MPs. (D) CP (blue = live cells; green = dead cells).

Thus, it was found that microencapsulation reduces the cytotoxicity of cyclophosphamide against healthy cells.

Conclusions

In this study, cyclophosphamide-loaded poly(3-hydroxybutyrate-co-3-hydroxyvalerate) microparticles were obtained and characterized. It was found that the loading of CP into PHBV microparticles leads to changes in the physical characteristics of the CP-containing formulation compared to the blank microparticles: the decrease of melting points and degradation temperature as well as increase of microparticles diameter, glass transition temperature and cold crystallization temperature were noted. Furthermore, *in vitro* cell viability assay revealed that the encapsulation of cyclophosphamide into PHBV microparticles decreased CP-MPs cytotoxicity against 3T3 cells compared to pure CP. In the future, in order to improve the uptake of the carrier by tumour cells, increase the residence in systemic circulation, facilitate particles' penetration into the interstitial space of the tumour via the EPR effect and circumvent premature

drug release, the obtained system can be modified. This can be accomplished by reducing the size of the particles, coating the particles' surfaces with a stealth shell, and functionalizing their surface with some ligands to provide active targeting and prevent macrophage uptake. Overall, this study offers promising prospects for cancer therapy in the future.

Supplementary material

Additional data are available at https://pub.iapchem.org/ojs/index.php/admet/article/view/2434, or from the corresponding author on request.

Acknowledgements: *NA*

Funding: *The study was funded by State Assignment of the Ministry of Science and Higher Education of the Russian Federation (project No. FWES-2021-0025).*

Conflict of interest: *Authors declare that there is no conflict of interest.*

Author Contributions: *All authors contributed to the study conception and design. Material preparation, data collection and analysis were performed by Sergei Lipaikin, Aleksei Dorokhin, Galina Ryltseva, Andrey Oberenko, Evgeniy Kiselev and Alexander Shabanov. Tatiana Volova and Ekaterina Shishatskaya supervised all phases of the study, including the manuscript writing. All authors read and approved the final manuscript.*

Data availability: *The authors confirm that the data supporting the findings of this study are available within the article. Any additional datasets are available from the corresponding author on reasonable request.*

Ethics approval and consent to participate: *NA*

Consent to participate: *NA*

Consent to publish: *NA*

References

[1] H. Arnold, F. Bourseaux, N. Brock. Chemotherapeutic Action of a Cyclic Nitrogen Mustard Phosphamide Ester (B 518-ASTA) in Experimental Tumours of the Rat. *Nature* **181** (1958) 931-931. https://doi.org/10.1038/181931a0.

[2] N. Helsby, M. Yong, K. Burns, M. Findlay, D. Porter. Cyclophosphamide bioactivation pharmacogenetics in breast cancer patients. *Cancer Chemotherapy and Pharmacology* **88** (2021) 533-542. https://doi.org/10.1007/s00280-021-04307-0.

[3] I. El-Serafi, S. Steele. Cyclophosphamide Pharmacogenomic Variation in Cancer Treatment and Its Effect on Bioactivation and Pharmacokinetics. *Advances in Pharmacological and Pharmaceutical Sciences* **2024** (2024) 862706. https://doi.org/10.1155/2024/4862706.

[4] E. Dabbish, S. Scoditti, M.N.I. Shehata, I. Ritacco, M.A.A. Ibrahim, T. Shoeib, E. Sicilia. Insights on cyclophosphamide metabolism and anticancer mechanism of action: A computational study. *Journal of Computational Chemistry* **45** (2024) 663-670. https://doi.org/10.1002/jcc.27280.

[5] J.J. Lokich, A. Bothe. Phase-I Study of Continuous Infusion Cyclophosphamide for Protracted Durations: A Preliminary Report. *Cancer Drug Delivery* **1** (1984) 329-332. https://doi.org/10.1089/cdd.1984.1.329.

[6] M.J. Moore. Clinical Pharmacokinetics of Cyclophosphamide. *Clinical Pharmacokinetics* **20** (1991) 194-208. https://doi.org/10.2165/00003088-199120030-00002.

[7] R. Samaritani, G. Corrado, E. Vizza, C. Sbiroli. Cyclophosphamide “metronomic” chemotherapy for palliative treatment of a young patient with advanced epithelial ovarian cancer. *BMC Cancer* **7** (2007) 65. https://doi.org/10.1186/1471-2407-7-65.

[8] M. Petri, R.A. Brodsky, R.J. Jones, D. Gladstone, M. Fillius, L.S. Magder. High-dose cyclophosphamide versus monthly intravenous cyclophosphamide for systemic lupus erythematosus: A prospective randomized trial. *Arthritis & Rheumatism* **62** (2010) 1487-1493. https://doi.org/10.1002/art.27371.

[9] Z. Cai, L. Gao, K. Hu, Q.-M. Wang. Parthenolide enhances the metronomic chemotherapy effect of cyclophosphamide in lung cancer by inhibiting the NF-kB signaling pathway. *World Journal of Clinical Oncology* **15** (2024) 895-907. https://doi.org/10.5306/wjco.v15.i7.895.

[10] S. Cetik Yildiz, C. Demir, M. Cengiz, H. Irmak, B.P. Cengiz, A. Ayhanci. In Vitro Antitumor and Antioxidant Capacity as well as Ameliorative Effects of Fermented Kefir on Cyclophosphamide-Induced Toxicity on Cardiac and Hepatic Tissues in Rats. *Biomedicines* **12** (2024) 1199. https://doi.org/10.3390/biomedicines12061199.

[11] T. Drie, M.I. Alsamman, R. Tarcha, G. Haidar, M. Kudsi. Successful pregnancy after cyclophosphamide therapy for systemic lupus erythematosus: a case report. *Annals of Medicine & Surgery* **86** (2024) 1156-1160. https://doi.org/10.1097/MS9.0000000000001641.

[12] S. Saracchini, L. Foltran, F. Tuccia, A. Bassini, S. Sulfaro, E. Micheli, A. Del Conte, M. Bertola, M. Gion, M. Lorenzon, S. Tumolo. Phase II study of liposome-encapsulated doxorubicin plus cyclophosphamide, followed by sequential trastuzumab plus docetaxel as primary systemic therapy for breast cancer patients with HER2 overexpression or amplification. *The Breast* **22** (2013) 1101-1107. https://doi.org/10.1016/j.breast.2013.09.001.

[13] K. Żółtowska, U. Piotrowska, E. Oledzka, U. Luchowska, M. Sobczak, A. Bocho-Janiszewska. Development of biodegradable polyesters with various microstructures for highly controlled release of epirubicin and cyclophosphamide. *European Journal of Pharmaceutical Sciences* **96** (2017) 440-448. https://doi.org/10.1016/j.ejps.2016.10.014.

[14] F. Abedin, M.R. Anwar, R. Asmatulu, S.-Y. Yang. Albumin-based micro-composite drug carriers with dual chemo-agents for targeted breast cancer treatment. *Journal of Biomaterials Applications* **30** (2015) 38-49. https://doi.org/10.1177/0885328215569614.

[15] A.A.Majeed, The assessment of Cyclophosphamide chemotherapy effect loading-PLGA nanoparticles against ovarian cancer cells line (OVCAR-4 & PEO1). *Journal of Pharmaceutical Negative Results* **13** (2022) 39-43. https://www.pnrjournal.com/index.php/home/article/view/180.

[16] Y.L. Ding, S.S. Ding, G.F. Ding. Preparation and Characterization of Cyclophosphamide-Loaded Chitosan Microspheres. *Advanced Materials Research* **621** (2012) 130-133. https://doi.org/10.4028/www.scientific.net/AMR.621.130.

[17] N.O. Zhila, K.Yu. Sapozhnikova, E.G. Kiselev, E.I. Shishatskaya, T.G. Volova. Biosynthesis of Polyhydroxyalkanoates in Cupriavidus necator B-10646 on Saturated Fatty Acids. *Polymers* **16** (2024) 1294. https://doi.org/10.3390/polym16091294.

[18] A. V. Murueva, A.E. Dudaev, E.I. Shishatskaya, F.D.E. Ghorabe, I. V. Nemtsev, A. V. Lukyanenko, T.G. Volova. Biodegradable polymer casting films for drug delivery and cell culture. *Giant* **19** (2024) 100314. https://doi.org/10.1016/j.giant.2024.100314.

[19] N.O. Zhila, E.G. Kiselev, V. V. Volkov, O.Ya. Mezenova, K.Yu. Sapozhnikova, E.I. Shishatskaya, T.G. Volova. Properties of Degradable Polyhydroxyalkanoates Synthesized from New Waste Fish Oils (WFOs). *International Journal of Molecular Sciences* **24** (2023) 14919. https://doi.org/10.3390/ijms241914919.

[20] L.Q. Fook, H.T. Tan, M. Lakshmanan, I. Zainab-L, A. Ahmad, S.L. Ang, K. Sudesh. Polyhydroxyalkanoate Biosynthesis from Waste Cooking Oils by Cupriavidus necator Strains Harbouring phaCBP-M-CPF4. *Journal of Polymers and the Environment* **32** (2024) 3490-3502. https://doi.org/10.1007/s10924-023-03166-5.

[21] S. Bano, A.A. Aslam, A. Khan, A. Shabbir, F. Qayyum, N. Wahab, A. Jabar, I. Ul Islam, S.L. Ng. A mini-review on polyhydroxyalkanoates: Synthesis, extraction, characterization, and applications. *Process Biochemistry* **146** (2024) 250-261. https://doi.org/10.1016/j.procbio.2024.07.033.

[22] R. Ma, J. Li, R. Tyagi, X. Zhang. Carbon dioxide and methane as carbon source for the production of polyhydroxyalkanoates and concomitant carbon fixation. *Bioresource Technology* **391** (2024) 129977. https://doi.org/10.1016/j.biortech.2023.129977.

[23] A.B. Kharissova, O. V. Kharissova, B.I. Kharisov, Y.P. Méndez. Carbon negative footprint materials: A review. *Nano-Structures & Nano-Objects* **37** (2024) 101100. https://doi.org/10.1016/j.nanoso.2024.101100.

[24] T.G. Volova, E.I. Shishatskaya, Cupriavidus eutrophus VKPM B-10646 Bacteria Strain — Producer of Polyhydroxyalkanoates and Production Method Thereof, RU2439143C1, 2012. https://patents.google.com/patent/RU2439143C1/en.

[25] Z.H. Mohamed, S.M. Amer, A.M. El-Kousasy. Colorimetric determination of cyclophosphamide and ifosphamide. *Journal of Pharmaceutical and Biomedical Analysis* **12** (1994) 1131-1136. https://doi.org/10.1016/0731-7085(94)E0020-2.

[26] A.P. Li, A. Uzgare, Y.S. LaForge. Definition of metabolism-dependent xenobiotic toxicity with co-cultures of human hepatocytes and mouse 3T3 fibroblasts in the novel integrated discrete multiple organ co-culture (IdMOC) experimental system: Results with model toxicants aflatoxin B1, cyclophosphamide and tamoxifen. *Chemico-Biological Interactions* **199** (2012) 1-8. https://doi.org/10.1016/j.cbi.2012.05.003.

[27] C.A. Schneider, W.S. Rasband, K.W. Eliceiri. NIH Image to ImageJ: 25 years of image analysis. *Nature Methods* **9** (2012) 671-675. https://doi.org/10.1038/nmeth.2089.

[28] S. Rodrigues, A. da Costa, N. Flórez-Fernández, M. Torres, M. Faleiro, F. Buttini, A. Grenha. Inhalable Spray-Dried Chondroitin Sulphate Microparticles: Effect of Different Solvents on Particle Properties and Drug Activity. *Polymers* **12** (2020) 425. https://doi.org/10.3390/polym12020425.

[29] G. Troiano, M. Figa, Abhimanyu Sabnis, Drug loaded polymeric nanoparticles and methods of making and using same, US 8.420,123 B2, 2013. https://patentimages.storage.googleapis.com/61/6c/13/c52dc4a0d5e5b2/US8420123.pdf

[30] J.K. Staas, T.R. Tice, B.W. Hudson, A. J. Tipton, Methods for manufacturing delivery devices and devices thereof, US 8,541,028 B2, 2013. https://patentimages.storage.googleapis.com/cd/73/7d/f88544b7ed22c4/US8541028.pdf

[31] A. Dorokhin, S. Lipaikin, G. Ryltseva, E. Shishatskaya, S.Kachin. Preparation and Characterization of Rifampicin-Loaded poly(3-hydroxybutyrate-co-3-hydroxyvalerate) Microparticles. *Journal of Siberian Federal University. Chemistry* **16(2)** (2023) 159-167. https://elib.sfu-kras.ru/bitstream/handle/2311/150144/01_Dorokhin.pdf

[32] F. Masood, P. Chen, T. Yasin, N. Fatima, F. Hasan, A. Hameed. Encapsulation of Ellipticine in poly-(3-hydroxybutyrate-co-3-hydroxyvalerate) based nanoparticles and its in vitro application. *Materials Science and Engineering: C* **33** (2013) 1054-1060. https://doi.org/10.1016/j.msec.2012.11.025.

[33] S. Lightfoot Vidal, C. Rojas, R. Bouza Padín, M. Pérez Rivera, A. Haensgen, M. González, S. Rodríguez-Llamazares. Synthesis and characterization of polyhydroxybutyrate- *co* -hydroxyvalerate nanoparticles for encapsulation of quercetin. *Journal of Bioactive and Compatible Polymers* **31** (2016) 439-452. https://doi.org/10.1177/0883911516635839.

[34] A. Shershneva, A. Murueva, E. Nikolaeva, E. Shishatskaya, T. Volova. Novel spray-dried PHA microparticles for antitumor drug release. *Drying Technology* **36** (2018) 1387-1398. https://doi.org/10.1080/07373937.2017.1407940.

[35] G.A. Senhorini, S.F. Zawadzki, P. V. Farago, S.M.W. Zanin, F.A. Marques. Microparticles of poly(hydroxybutyrate-co-hydroxyvalerate) loaded with andiroba oil: Preparation and characterization. *Materials Science and Engineering: C* **32** (2012) 1121-1126. https://doi.org/10.1016/j.msec.2012.02.027.

[36] A.V. Vladimirova, A. V. Murueva, A. M. Shershneva, S.V. Prudnikova, A.V. Shabanov, E.I. Shishatskaya. Biocompatible Systems for Controlled Delivery of Antiseptics for Topical Application. *Journal of Siberian Federal University. Biology* **17** (2024) 19-32. https://elib.sfu-kras.ru/bitstream/handle/2311/152806/02_Vladimirova.pdf?sequence=1

[37] M.E. de Jonge, A.D.R. Huitema, S. Rodenhuis, J.H. Beijnen. Clinical Pharmacokinetics of Cyclophosphamide. *Clinical Pharmacokinetics* **44** (2005) 1135-1164. https://doi.org/10.2165/00003088-200544110-00003.

[38] Y. Zhang, S. Fei, M. Yu, Y. Guo, H. He, Y. Zhang, T. Yin, H. Xu, X. Tang. Injectable sustained release PLA microparticles prepared by solvent evaporation-media milling technology. *Drug Development and Industrial Pharmacy* **44** (2018) 1591-1597. https://doi.org/10.1080/03639045.2018.1483382.

[39] E. Yapar, Ö. İnal, Y. Özkan, T. Baykara. Injectable In Situ Forming Microparticles: A Novel Drug Delivery System. *Tropical Journal of Pharmaceutical Research* **11** (2012) 307-318. https://doi.org/10.4314/tjpr.v11i2.19.

[40] A. Cambronero-Rojas, P. Torres-Vergara, R. Godoy, C. von Plessing, J. Sepúlveda, C. Gómez-Gaete. Capreomycin oleate microparticles for intramuscular administration: Preparation, in vitro release and preliminary in vivo evaluation. *Journal of Controlled Release* **209** (2015) 229-237. https://doi.org/10.1016/j.jconrel.2015.05.001.

[41] E.I. Shishatskaya, O.N. Voinova, A. V. Goreva, O.A. Mogilnaya, T.G. Volova. Tissue reaction to intramuscular injection of resorbable polymer microparticles. *Bulletin of Experimental Biology and Medicine* **144** (2007) 786-790. https://doi.org/10.1007/s10517-007-0432-0.

[42] S.P. Schwendeman, R.B. Shah, B.A. Bailey, A.S. Schwendeman. Injectable controlled release depots for large molecules. *Journal of Controlled Release* **190** (2014) 240-253. https://doi.org/10.1016/j.jconrel.2014.05.057.

[43] R.L. Juliano. Factors affecting the clearance kinetics and tissue distribution of liposomes, microspheres and emulsions. *Advanced Drug Delivery Reviews* **2** (1988) 31-54. https://doi.org/10.1016/0169-409X(88)90004-X.

[44] D. Liu, D.T. Auguste. Cancer targeted therapeutics: From molecules to drug delivery vehicles. *Journal of Controlled Release* **219** (2015) 632-643. https://doi.org/10.1016/j.jconrel.2015.08.041.

[45] A. Kumar, C.K. Dixit. Methods for characterization of nanoparticles. in: Advances in Nanomedicine for the Delivery of Therapeutic Nucleic Acids, Elsevier, 2017: p. 43-58. https://doi.org/10.1016/B978-0-08-100557-6.00003-1.

[46] A.M. Shershneva, A. V. Murueva, E.I. Shishatskaya, T.G. Volova. Study of electrokinetic potential of drug micro-carriers prepared from resorbable polymers bioplastotan. *Biophysics* **59** (2014) 561-567. https://doi.org/10.1134/S000635091404023X.

[47] R. Singh, J.W. Lillard. Nanoparticle-based targeted drug delivery. *Experimental and Molecular Pathology* **86** (2009) 215-223. https://doi.org/10.1016/j.yexmp.2008.12.004.

[48] I. Corrado, R. Di Girolamo, C. Regalado-González, C. Pezzella. Polyhydroxyalkanoates-Based Nanoparticles as Essential Oil Carriers. *Polymers* **14** (2022) 166. https://doi.org/10.3390/polym14010166.

[49] A. V. Murueva, A.M. Shershneva, I. V. Nemtsev, E.I. Shishatskaya, T.G. Volova. Collagen conjugation to carboxyl-modified poly(3-hydroxybutyrate) microparticles: preparation, characterization and evaluation in vitro. *Journal of Polymer Research* **29** (2022). https://doi.org/10.1007/s10965-022-03181-5.

[50] S.Y. Lipaikin, I.A. Yaremenko, A.O. Terent'ev, T.G. Volova, E.I. Shishatskaya. Development of Biodegradable Delivery Systems Containing Novel 1,2,4-Trioxolane Based on Bacterial

Polyhydroxyalkanoates. *Advances in Polymer Technology* **2022** (2022) 6353909. https://doi.org/10.1155/2022/6353909.

[51] Q. Xu, A. Crossley, J. Czernuszka. Preparation and characterization of negatively charged poly(lactic-co-glycolic acid) microspheres. *Journal of Pharmaceutical Sciences* **98** (2009) 2377-2389. https://doi.org/10.1002/jps.21612.

[52] G. Ruan, S.-S. Feng. Preparation and characterization of poly(lactic acid)-poly(ethylene glycol)-poly(lactic acid) (PLA-PEG-PLA) microspheres for controlled release of paclitaxel. *Biomaterials* **24** (2003) 5037-5044. https://doi.org/10.1016/S0142-9612(03)00419-8.

[53] A.M. Shershneva, A. V. Murueva, N.O. Zhila, T.G. Volova. Antifungal activity of P3HB microparticles containing tebuconazole. *Journal of Environmental Science and Health, Part B* **54** (2019) 196-204. https://doi.org/10.1080/03601234.2018.1550299.

[54] E. Campos, J. Branquinho, A.S. Carreira, A. Carvalho, P. Coimbra, P. Ferreira, M.H. Gil. Designing polymeric microparticles for biomedical and industrial applications. *European Polymer Journal* **49** (2013) 2005-2021. https://doi.org/10.1016/j.eurpolymj.2013.04.033.

[55] D. Sendil, I. Gürsel, D. L. Wise, V. Hasırcı. Antibiotic release from biodegradable PHBV microparticles. *Journal of Controlled Release* **59** (1999) 207-217. https://doi.org/10.1016/S0168-3659(98)00195-3.

[56] W. Huang, Y. Wang, L. Ren, C. Du, X. Shi. A novel PHBV/HA microsphere releasing system loaded with alendronate. *Materials Science and Engineering: C* **29** (2009) 2221-2225. https://doi.org/10.1016/j.msec.2009.05.015.

[57] N. Pettinelli, S. Rodríguez-Llamazares, Y. Farrag, R. Bouza, L. Barral, S. Feijoo-Bandín, F. Lago. Poly(hydroxybutyrate-co-hydroxyvalerate) microparticles embedded in κ-carrageenan/locust bean gum hydrogel as a dual drug delivery carrier. *International Journal of Biological Macromolecules* **146** (2020) 110-118. https://doi.org/10.1016/j.ijbiomac.2019.12.193.

[58] C. Zhang, Y. Dong, L. Zhao. Preparation and characterization of novel microparticles based on poly(3-hydroxybutyrate-co-3-hydroxyoctanoate). *Journal of Microencapsulation* **31** (2014) 9-15. https://doi.org/10.3109/02652048.2013.799241.

[59] B. Remila, I. Zembouai, L. Zaidi, A. Alane, M. Kaci, A. Kervoelen, S. Bruzaud. Investigations on structure and properties of poly (3-hydroxybutyrate-co-3-hydroxyvalerate) (PHBV) reinforced by diss fibers: Effect of various surface treatments. *Industrial Crops and Products* **221** (2024) 119302. https://doi.org/10.1016/j.indcrop.2024.119302.

[60] Z. Keshtmand, S.N. Naimi, Z. Koureshi Piran, P. Poorjafari Jafroodi, M. Tavakkoli Yaraki. Enhanced anticancer effect of Artemisia turcomanica extract in niosomal formulation on breast cancer cells: In-vitro study. *Nano-Structures & Nano-Objects* **35** (2023) 101030. https://doi.org/10.1016/j.nanoso.2023.101030.

[61] L. Li, L. Jing, Z. Tang, J. Du, Y. Zhong, X. Liu, M. Yuan. Dual-targeting liposomes modified with BTP-7 and pHA for combined delivery of TCPP and TMZ to enhance the anti-tumour effect in glioblastoma cells. *Journal of Microencapsulation* **41** (2024) 419-433. https://doi.org/10.1080/02652048.2024.2376114.

[62] Z. Salmasi, H. Kamali, H. Rezaee, F. Nazeran, Z. Jafari, F. Eisvand, M. Teymouri, E. Khordad, J. Mosafer. Simultaneous therapeutic and diagnostic applications of magnetic PLGA nanoparticles loaded with doxorubicin in rabbit. *Drug Delivery and Translational Research* (2024). https://doi.org/10.1007/s13346-024-01693-9.

[63] S. Sur, A. Rathore, V. Dave, K.R. Reddy, R.S. Chouhan, V. Sadhu. Recent developments in functionalized polymer nanoparticles for efficient drug delivery system. *Nano-Structures & Nano-Objects* **20** (2019) 100397. https://doi.org/10.1016/j.nanoso.2019.100397.

[64] A. Estrada-Monje, M.A. Silva-Goujon, I. Rodríguez-Sánchez, A.S. Conejo-Dávila, C.I. Piñón-Balderrama, A. Zaragoza-Estrada, L.A. Baldenegro-Pérez, E.A. Zaragoza-Contreras. Effect of the Addition of PLA on the Thermal and Mechanical Properties of Reprocessed HDPE. *Polymers* **16** (2024) 2387. https://doi.org/10.3390/polym16162387.

[65] N. Zafar, A. Mahmood, R.M. Sarfraz, H. Ijaz, M.U. Ashraf, S. Mehr. Facile synthesis of β-cyclodextrin-cyclophosphamide complex-loaded hydrogel for controlled release drug delivery. *Polymer Bulletin* **80** (2023) 10939-10971. https://doi.org/10.1007/s00289-022-04567-7.

[66] P. Kommavarapu, A. Maruthapillai, A. Ravikiran, P. Kamaraj. Sorption-Desorption Behavior and Characterization of Cyclophosphamide. *Chemical Science Transactions* **2** (2013). http://www.e-journals.in/pdf/v2ns1/s135-s140.pdf.

[67] N.O. Zhila, K.Yu. Sapozhnikova, E.G. Kiselev, E.I. Shishatskaya, T.G. Volova. Synthesis and Properties of Polyhydroxyalkanoates on Waste Fish Oil from the Production of Canned Sprats. *Processes* **11** (2023) 2113. https://doi.org/10.3390/pr11072113.

[68] C.C. Nwazojie, J.D. Obayemi, A.A. Salifu, S.M. Borbor-Sawyer, V.O. Uzonwanne, C.E. Onyekanne, U.M. Akpan, K.C. Onwudiwe, J.C. Oparah, O.S. Odusanya, W.O. Soboyejo. Targeted drug-loaded PLGA-PCL microspheres for specific and localized treatment of triple negative breast cancer. *Journal of Materials Science: Materials in Medicine* **34** (2023) 41. https://doi.org/10.1007/s10856-023-06738-y.

[69] S.M. Jusu, J.D. Obayemi, A.A. Salifu, C.C. Nwazojie, V. Uzonwanne, O.S. Odusanya, W.O. Soboyejo. Drug-encapsulated blend of PLGA-PEG microspheres: in vitro and in vivo study of the effects of localized/targeted drug delivery on the treatment of triple-negative breast cancer. *Scientific Reports* **10** (2020) 14188 . https://doi.org/10.1038/s41598-020-71129-0.

[70] P. V. Farago, R.P. Raffin, A.R. Pohlmann, S.S. Guterres, S.F. Zawadzki. Physicochemical characterization of a hydrophilic model drug-loaded PHBV microparticles obtained by the double emulsion/solvent evaporation technique. *Journal of the Brazilian Chemical Society* **19** (2008) 1298-1305. https://doi.org/10.1590/S0103-50532008000700011.

[71] M.K. Sahu, N. Dubey, R. Pandey, S.S. Shukla, B. Gidwani. Formulation, Evaluation, and Validation of Microspheres of Cyclophosphamide for Topical Delivery. *Pharmacophore* **14** (2023) 1-8. https://doi.org/10.51847/e4GvuoN96z.

[72] A. V. Murueva, A.M. Shershneva, K. V. Abanina, S. V. Prudnikova, E.I. Shishatskaya. Development and characterization of ceftriaxone-loaded P3HB-based microparticles for drug delivery. *Drying Technology* **37** (2019) 1131-1142. https://doi.org/10.1080/07373937.2018.1487451.

[73] E.G. Kiselev, S. V. Baranovskiy. The Kinetics of Fungicide and Herbicide Release from Slow-Release Formulations Prepared from Degradable Poly-3- Hydroxybutyrate. *Journal of Siberian Federal University. Biology* **9** (2016) 233-240. https://doi.org/10.17516/1997-1389-2016-9-2-233-240.

[74] T.G. Volova, A. V. Demidenko, A. V. Murueva, A.E. Dudaev, I. Nemtsev, E.I. Shishatskaya. Biodegradable Polyhydroxyalkanoates Formed by 3- and 4-Hydroxybutyrate Monomers to Produce Nanomembranes Suitable for Drug Delivery and Cell Culture. *Technologies* **11** (2023) 106. https://doi.org/10.3390/technologies11040106.

[75] A. V. Murueva, A.M. Shershneva, E.I. Shishatskaya, T.G. Volova. Characteristics of Microparticles Based on Resorbable Polyhydroxyalkanoates Loaded with Antibacterial and Cytostatic Drugs. *International Journal of Molecular Sciences* **24** (2023) 14983. https://doi.org/10.3390/ijms241914983.

[76] K. Ghosal, A. Das, S.K. Das, S. Mahmood, M.A.M. Ramadan, S. Thomas. Synthesis and characterization of interpenetrating polymeric networks based bio-composite alginate film: A well-designed drug delivery platform. *International Journal of Biological Macromolecules* **130** (2019) 645-654. https://doi.org/10.1016/j.ijbiomac.2019.02.117.

[77] K.S. Joshy, M.A. Susan, S. Snigdha, K. Nandakumar, A.P. Laly, T. Sabu. Encapsulation of zidovudine in PF-68 coated alginate conjugate nanoparticles for anti-HIV drug delivery. *International Journal of Biological Macromolecules* **107** (2018) 929-937. https://doi.org/10.1016/j.ijbiomac.2017.09.078.

[78] K.S. Joshy, A. George, J. Jose, N. Kalarikkal, L.A. Pothen, S. Thomas. Novel dendritic structure of alginate hybrid nanoparticles for effective anti-viral drug delivery. *International Journal of Biological Macromolecules* **103** (2017) 1265-1275. https://doi.org/10.1016/j.ijbiomac.2017.05.094.

[79] N. Durán, M.A. Alvarenga, E.C. Da Silva, P.S. Melo, P.D. Marcato. Microencapsulation of antibiotic rifampicin in poly(3-hydroxybutyrate-co-3-hydroxyvalerate). *Archives of Pharmacal Research* **31** (2008) 1509-1516. https://doi.org/10.1007/s12272-001-2137-7.

[80] L. Nair, J. Sankar, S.A. Nair, G.V. Kumar. Biological evaluation of 5-fluorouracil nanoparticles for cancer chemotherapy and its dependence on the carrier, PLGA. *International Journal of Nanomedicine* (2011) 1685-1697. https://doi.org/10.2147/IJN.S20165